

# Room-Temperature Ni Interaction with Deformation-Induced Defects in Si: A DLTS Study

Oleg A. Soltanovich, Valery I. Orlov, Nikolai Yarykin, and Eugene B. Yakimov\*

The deep-level (DL) spectrum of plastically deformed n-type Si and its modification due to interaction with the mobile Ni species are investigated by the deep-level transient spectroscopy (DLTS) technique. The used geometry of plastic deformation makes it possible to separate the DL centers associated with the dislocations themselves or with dislocation traces, the quasi-2D defects left by moving dislocations. It is shown that the chemomechanical polishing at room temperature in a Ni-contaminated slurry results in the appearance of additional DL centers; the principal part of the novel centers forms due to nickel interaction with the dislocation trails. The DLTS signatures of the nickel-related defects in our plastically deformed samples are similar to those for the nickel-silicide precipitates.

## 1. Introduction

The interaction of transition metals (TMs) with extended defects is one of the key issues that need to be understood for optimization of the gettering procedures in the solar-grade Si, which is known to contain iron, copper, and nickel in rather high concentrations. In the as-grown state, these impurities are mainly precipitated and have a limited impact on the semiconductor parameters. However, the precipitates could be (partially) dissolved during the solar-cell processing, which transforms the impurities into the interstitial state. The interstitial impurities are mobile already at room temperature and can interact with the extended defects. In model experiments, these processes are simulated by introduction of the TM impurities into the plastically deformed high-quality crystals.<sup>[1–11]</sup>

Plastic deformation of Si crystals at 600–700 °C is known to introduce, along with dislocations, another type of extended defects, the so-called dislocation trails (DTs).<sup>[12–17]</sup> Although their nature is still vague, the DTs were shown to introduce levels in the Si bandgap. DTs are quasi-2D defects that are formed in the part of the dislocation slip plane swept by the dislocation. Using the beam-injection techniques, such as electron-beam-induced current (EBIC) or light-beam-induced current (LBIC), the

recombination strength of trails and dislocations can be estimated separately. However, these methods are unable to provide a detailed information about the spectrum of the energy levels related to those defects. In contrast, the spectroscopic techniques, such as deep-level transient spectroscopy (DLTS), give a combined picture determined by both the defect types. In this work, we have managed to distinguish the DLTS signals from dislocations and DTs using a special geometry of the plastic deformation.

Electrical activity of both dislocations and DTs was reported to depend on contamination with TMs.<sup>[2,7,9–11,18]</sup> In those

experiments, the plastic deformation was usually performed at temperatures around 700 °C, whereas the metals were then introduced at similar or higher temperatures. Such thermal treatments are known to influence the DL spectrum of the plastically deformed Si also in the cases when there was no deliberate contamination.<sup>[13,15,19]</sup> Therefore, it is of great interest to distinguish the effects of annealing and contamination.

Some TMs, such as copper, nickel, and iron, can diffuse over long distances at temperatures much lower than those usually used for plastic deformation. However, their solubilities drop down quickly at lower temperatures that prevents introduction of a measurable amount of metals. It was recently demonstrated that the chemomechanical polishing (CMP) in the Ni-contaminated alkaline slurry can introduce Ni up to concentration orders of magnitude higher than the equilibrium solubility.<sup>[20]</sup> In the following, we investigate how the room-temperature Ni incorporation affects the DL spectrum of plastically deformed Si.


## 2. Experimental Section

It was recently revealed that the DTs were formed behind moving dislocations of the particular type only, namely, those 60° segments, where the 90° and 30° Shockley partials were leading and trailing, respectively.<sup>[21,22]</sup> Therefore, the DT location inside an expanding dislocation loop depended on the deformation geometry.

The samples for the four-point bending around the  $\langle 110 \rangle$  axis were cut from the dislocation-free n-type Cz-Si crystal ( $[P] = 3 \times 10^{14} \text{ cm}^{-3}$ ) so that the wide working (top and bottom) surfaces had the  $\{1\ 0\ 0\}$  orientation (Figure 1). The dislocation half-loops nucleated at the intentionally made scratches were expanded from the top and bottom surfaces in two equivalent  $\{1\ 1\ 1\}$  planes (only one shown in Figure 1) under the compressive or tensile stresses, respectively. Plastic deformation was

O. A. Soltanovich, Dr. V. I. Orlov, Dr. N. Yarykin, Prof. E. B. Yakimov  
Institute of Microelectronics Technology RAS  
Chernogolovka 142432, Russia  
E-mail: yakimov@iptm.ru

Dr. V. I. Orlov  
Institute of Solid State Physics RAS  
Chernogolovka 142432, Russia

 The ORCID identification number(s) for the author(s) of this article can be found under <https://doi.org/10.1002/pssa.201900326>.

DOI: 10.1002/pssa.201900326

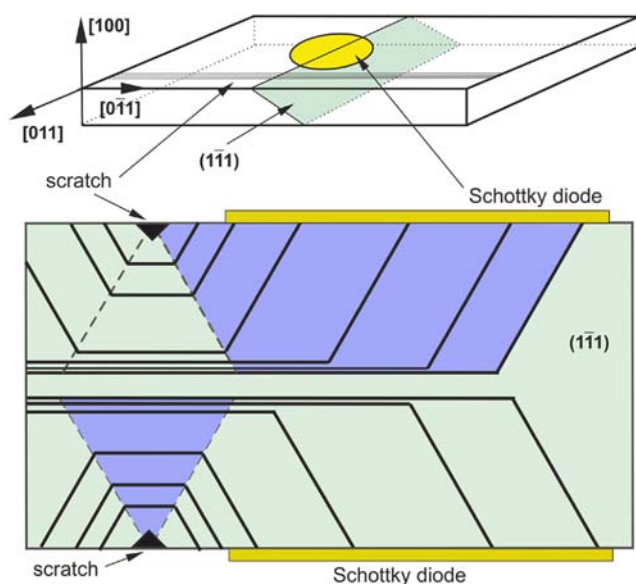


**Figure 1.** Plastic deformation scheme (at top) and sketch of the defect distribution in the  $(1\bar{1}1)$  plane after the four-point bending around the  $[0\ 1\ 1]$  axis. Thick lines correspond to the dislocation half-loops. The areas where the DTs were expected to form are shaded. DLTS signals were taken in a narrow layer below the Schottky diodes.

performed at  $600^\circ\text{C}$  under the resolved shear stress of about 40 MPa, resulting in the dislocation half-loops up to 3.5–4 mm in diameter. Such procedure ensured a rather uniform dislocation density of  $(1.5\text{--}5) \times 10^5\text{ cm}^{-2}$ , as obtained by counting the etch pits over the working surfaces.

For the given sample orientation, all dislocation half-loops had the  $60^\circ$  bottom segment and the arms of the  $60^\circ$  and screw type. The splitting of the perfect  $60^\circ$  dislocation during plastic deformation into Shockley partials was governed by the condition that the stacking fault between the partials was of intrinsic type.<sup>[23]</sup> It was easy to find that the  $90\text{--}30^\circ$  order of partials was always realized for the  $60^\circ$  arms at the top (compressive) surface and for the bottom segment at the opposite side. The above consideration was confirmed by the observation of DTs in the samples of given orientation by the EBIC and LBIC techniques.<sup>[22,24]</sup>

DLTS spectra were measured using the Schottky diodes fabricated on the working surfaces. The analyzed depth of the DLTS technique was determined by the width of the diode depletion region under the reverse bias. For the samples under study, it was about  $9\ \mu\text{m}$  under the maximum reverse bias of 18 V, i.e., always small as compared with the size of the dislocation half-loops. Therefore, the DLTS signals were mainly determined by the threading  $60^\circ$  and screw dislocations at the bottom surface and by a combination of the dislocations and the DTs at the top side (Figure 1).

### 3. Sample Preparation

The CMP was conducted on a laboratory scale. The commercially available silica-based slurry (density of  $1.39\text{ g mL}^{-1}$ ) was ten times diluted with a 20% KOH aqueous solution, resulting in

the material removal rate about  $0.1\text{--}0.5\ \mu\text{m min}^{-1}$  with the characteristic polishing time of  $\approx 10\text{ min}$ . The CMP procedure under these conditions led to no significant changes of the DLTS spectra of plastically deformed silicon measured after the standard wet chemical etching in CP4 acid solution.

The mobile Ni species were introduced by CMP in the slurry, which was deliberately contaminated by adding a small amount of diluted nitric acid in which a piece of pure nickel was dissolved. The final metal concentration in the slurry was about  $100\ \mu\text{g mL}^{-1}$ . The resulted pH-factor of the solution was always above 10.

The Schottky diodes for DLTS studies were fabricated by vacuum evaporation of gold through a shadow mask. The ohmic contacts were made by rubbing the opposite surface of the sample with a Ga–Al paste. The DL spectra were measured in the temperature range from 80 to 300 K using a standard DLTS setup with the square-wave lock-in amplifier as a correlator. Unless otherwise mentioned, the filling pulse duration of 1 ms and the rate window of  $53\text{ s}^{-1}$  were used. Most of the DLTS spectra were measured under the steady-state reverse bias of 9.5 V and filling-pulse amplitude of 6 V to avoid possible effects related to the surface. According to the CV characteristics, a layer of  $3.3\text{--}5.5\ \mu\text{m}$  was probed under these conditions.

### 4. Results and Discussion

The DLTS spectra shown in **Figure 2** were measured using the Schottky diodes located on the top and bottom  $\{1\ 0\ 0\}$  sample surfaces, which were subjected to the plastic deformation at  $600^\circ\text{C}$  under the compressive and tensile stresses, respectively. Although the dislocation densities under the diodes differed not more than by 30–40%, the spectra were essentially different.

At the tensile surface, the DL spectrum resembles that known as “dislocation-related” from many previous studies.<sup>[19,25,26]</sup> The positions of the B and D peaks perfectly conform to the corresponding Arrhenius lines from the studies by Omling et al.,<sup>[26]</sup> and the C peak agrees well with the  $\text{DE}_2$  feature from the studies

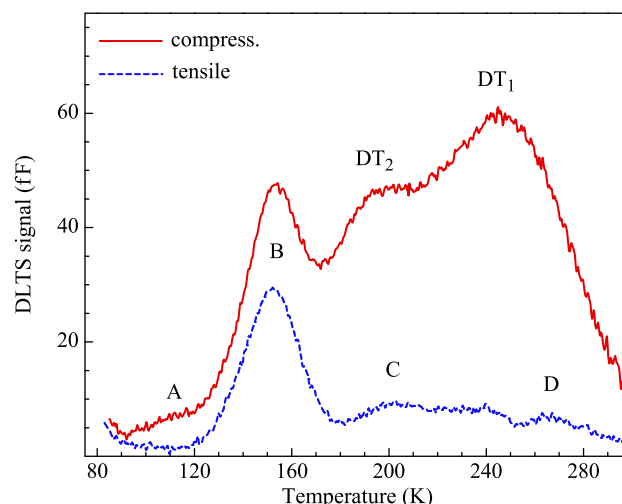


**Figure 2.** DLTS spectra measured at the compressive (solid curve) and tensile (dashed curve)  $\{1\ 0\ 0\}$  surfaces after the plastic deformation at  $600^\circ\text{C}$ .

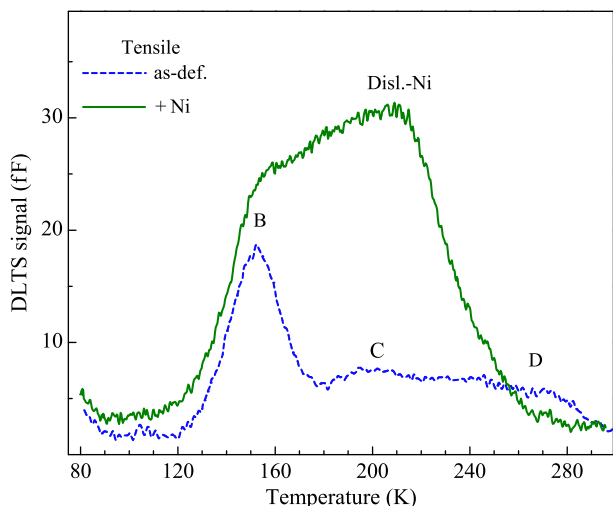


**Figure 3.** DLTS spectra measured at the tensile side of plastically deformed sample before (dashed curve) and after (solid curve) the CMP in the Ni-contaminated slurry.

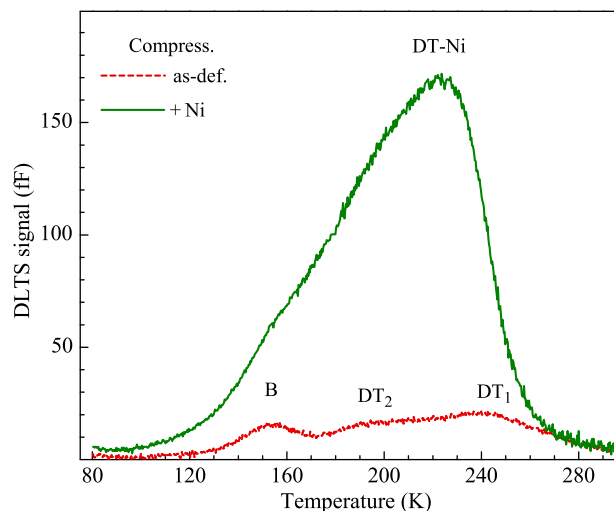


**Figure 4.** DLTS spectra measured at the compressive side of plastically deformed sample before (dashed curve) and after (solid curve) the CMP in the Ni-contaminated slurry.

by Kveder et al.<sup>[25]</sup> At the top surface, the DLTS spectrum looks like a superposition of the dislocation-related one and a broad double-humped feature. As DTs are known to introduce recombination centers, we related the additional signal with the DTs, and the two maxima at  $T_m \approx 245$  K and  $T_m \approx 190$  K are labeled as DT<sub>1</sub> and DT<sub>2</sub>, respectively (Figure 2). A similar (but much weaker) spectrum was earlier also attributed to DTs.<sup>[14]</sup> Note that the DT<sub>1</sub> peak coincides neither with the C<sub>2</sub> nor with the D features.<sup>[26]</sup> It is not clear at the moment if the DT<sub>2</sub> and C lines correspond to the same defect.

#### 4.1. Contamination with Ni

Another set of samples with a slightly lower density of dislocations and DTs was prepared to study the impact of nickel. Still, the dashed curves in Figure 3 and 4, which were measured before the Ni introduction at the bottom and top surfaces, respectively, reproduce well the main features seen in Figure 2.

The DL spectra at both sides were essentially changed after contamination with Ni. At the tensile side, a broad asymmetrical peak with  $T_m \approx 210$  K appeared in the DLTS spectrum, whereas the B-line remained primarily unaffected (Figure 3). The labeling of the novel broad feature implies that the DTs were absent at the bottom surface, and the signal was determined by the nickel interaction with dislocations only. Note that the Disl.-Ni peak position closely corresponds to the C<sub>1</sub> line, which was attributed to dislocations.<sup>[26]</sup>

Much more drastic changes due to incorporation of Ni were observed at the compressive side (Figure 4). A novel broad feature with  $T_m \approx 225$  K was almost an order of magnitude higher than the DLTS signal before the Ni in-diffusion. Nothing can be stated about the pre-existed features as well as about the Disl.-Ni signal in this case because they were totally hidden under the strong DT-Ni peak (see the ordinate scales in Figure 3 and 4). The DT-Ni peak position is close to the C<sub>2</sub> line.<sup>[26]</sup> Note also that the DLTS peak due to the acceptor level of

substitutional nickel atom would be expected at  $\approx 230$  K under our conditions.<sup>[27,28]</sup> However, special assumptions are required to explain how a broad DLTS feature like DT-Ni could be produced by point defects.

The amplitudes of all DLTS peaks observed after the Ni incorporation exhibit logarithmic dependences on the filling-pulse duration  $t_p$ , which was varied by more than four orders of magnitude (Figure 5). Note that occupation of the DT-Ni and Disl.-Ni traps increases by approximately two times in the considered  $t_p$  range, whereas filling of the B traps is increased by a factor of five.

The linear dependence of the DLTS peak amplitudes on  $\log(t_p)$  is commonly accepted as indication of an extended nature of the

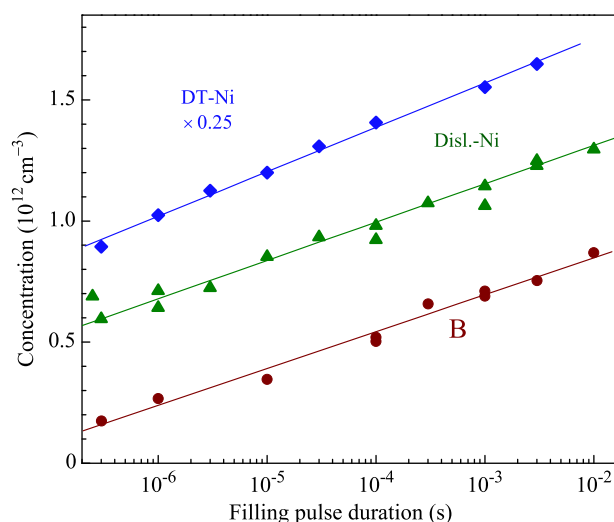


**Figure 5.** Concentration of the electrons trapped to the centers B (dots) and Disl.-Ni (triangles) at the tensile side and to the centers DT-Ni at the compressive side (diamonds) as a function of the filling-pulse duration. The straight lines are best fits to the data.

corresponding defects. The underlying reason for such behavior is the formation of an electrostatic barrier  $e\Phi$  around the defect due to the capture of majority carriers.<sup>[29]</sup> For 1D defects (dislocations),  $e\Phi \propto f$ , where  $f$  is the trap-filling factor.<sup>[25,26]</sup> It can be shown that, for 2D and 3D extended defects, this dependence is slower for smaller  $f$  (e.g.,  $e\Phi \propto f^2$  for a 2D defect). Simulations show that the  $f$  versus  $\log(t_p)$  dependence in this case is also very close to linear but reaches  $\approx 50\%$  of its maximum already at the shortest used pulses. Based on this consideration and taking into account the relatively higher amplitudes of the Ni-related defects at shorter pulses, one could assume that the Disl.-Ni and DT-Ni signals are determined by nickel precipitates formed at dislocations or DTs, respectively.

Thus, the effect of Ni in-diffusion is much stronger at the compressive surface. As the only difference between the top and bottom surfaces consisted in the presence of DTs, the dominating signal in Figure 4 has to be attributed to an interaction between nickel and the DTs. The same conclusion was drawn from analysis of the EBIC and LBIC contrasts in similar samples contaminated with Ni.<sup>[24]</sup> These results are in contradiction with the report that nickel interacts with dislocations only and not with the DTs.<sup>[10,11]</sup> In those studies, the plastically deformed samples were first subjected to Al gettering at 830 °C, and then, nickel was introduced by diffusion at 600 °C. Clearly, the high-temperature treatments could modify the DT properties. Also, the binding between Ni and DTs could be unstable at higher temperatures.

In conclusion, it is found that the room-temperature Ni incorporation into the plastically deformed Si results in the formation of additional DL centers which DLTS peaks appear in the 190–225 K range. The most abundant centers are formed due to a Ni reaction with the DTs. The structure of the Ni-related complexes in the plastically deformed Si is not clear at the moment. However, we note that the DLTS peak positions of these centers are well correlated with the interval where the DLTS signatures of the nanoscale NiSi<sub>2</sub> platelets were found.<sup>[30]</sup>

## Acknowledgements

The work in IMT RAS was performed in frames of the state task No 075-00475-19-00. The work in ISSP RAS was done as a part of the state task of ISSP RAS.

## Conflict of Interest

The authors declare no conflict of interest.

## Keywords

deep levels, dislocation trails, nickel, silicon

Received: April 16, 2019

Revised: July 1, 2019

Published online:

- [1] E. R. Weber, *Appl. Phys. A* **1983**, 30, 1.
- [2] M. Kittler, C. Ulhaq-Bouillet, V. Higgs, *Mater. Sci. Engineer. B* **1994**, 24, 52.
- [3] J. Jablonski, J. Kaniewski, M. Kaniewska, T. Sekiguchi, L. Ornoch, K. Sumino, *Mater. Sci. Forum* **1994**, 143–147, 1517.
- [4] P. R. Wilshaw, T. S. Fell, *J. Electrochem. Soc.* **1995**, 142, 4298.
- [5] B. Shen, T. Sekiguchi, R. Zhang, Y. Shi, H. Shi, K. Yang, Y. D. Zheng, K. Sumino, *Jpn. J. Appl. Phys.* **1996**, 35, 3301.
- [6] W. Schröter, M. Seibt, D. Gilles, In *Handbook of Semiconductor Technology* (Eds: K. A. Jackson, W. Schröter), Wiley-VCH Verlag GmbH, Weinheim **2000**, p. 597.
- [7] M. Seibt, V. Kveder, W. Schröter, O. Voß, *Phys. Status Solidi A* **2005**, 202, 911.
- [8] O. V. Feklisova, E. B. Yakimov, *Phys. Solid State* **2011**, 53, 1240.
- [9] M. Khorosheva, V. V. Kveder, M. Seibt, *Phys. Status Solidi A* **2015**, 212, 1695.
- [10] V. V. Kveder, M. Khorosheva, M. Seibt, *Solid State Phenom.* **2016**, 242, 147.
- [11] V. Kveder, M. Khorosheva, M. Seibt, *Mater. Today: Proc.* **2018**, 5, 14757.
- [12] I. Bondarenko, V. G. Eremenko, B. Farber, V. I. Nikitenko, E. B. Yakimov, *Phys. Status Solidi A* **1981**, 68, 53.
- [13] I. Bondarenko, H. Blumtritt, J. Heydenreich, V. V. Kazmiruk, E. B. Yakimov, *Phys. Status Solidi A* **1986**, 95, 173.
- [14] E. B. Yakimov, I. Bondarenko, N. Yarykin, *Mater. Sci. Forum* **1986**, 10–12, 787.
- [15] O. V. Feklisova, E. B. Yakimov, N. Yarykin, *Phys. B* **2003**, 340–342, 1005.
- [16] D. Eyidi, V. Eremenko, J. L. Dermenet, J. Rabier, *Phys. B* **2009**, 404, 4634.
- [17] J. Rabier, L. Pizzagalli, *J. Phys.: Conf. Ser.* **2011**, 281, 012025.
- [18] O. V. Feklisova, E. B. Yakimov, *Semiconductors* **2015**, 49, 716.
- [19] D. Cavalcoli, A. Cavallini, E. Gombia, *Phys. Rev. B* **1997**, 56, 10208.
- [20] N. Yarykin, J. Weber, *Phys. Status Solidi C* **2017**, 14, 1700005.
- [21] V. I. Orlov, E. B. Yakimov, N. Yarykin, *Solid State Phenom.* **2016**, 242, 155.
- [22] V. I. Orlov, E. B. Yakimov, N. Yarykin, *Phys. Status Solidi C* **2017**, 14, 1700074.
- [23] J. P. Hirth, J. Lothe, *Theory of Dislocations*, John Wiley & Sons, New York **1982**.
- [24] V. I. Orlov, N. Yarykin, E. B. Yakimov, *Semiconductors* **2019**, 53, 433.
- [25] V. V. Kveder, Y. A. Ossipyan, W. Schröter, G. Zoth, *Phys. Status Solidi A* **1982**, 72, 701.
- [26] P. Omeling, E. R. Weber, L. Montelius, H. Alexander, J. Michel, *Phys. Rev. B* **1985**, 32, 6571.
- [27] H. Lemke, *Phys. Status Solidi A* **1987**, 99, 205.
- [28] L. Scheffler, V. Kolkovsky, J. Weber, *J. Appl. Phys.* **2014**, 116, 173704.
- [29] T. Figielski, *Solid-State Electron.* **1978**, 21, 1403.
- [30] F. Riedel, W. Schröter, *Phys. Rev. B* **2000**, 62, 7150.